Electrochemical synthesis of poly(trisulfides)

Jasmine M. M. Pople,[1] Thomas P. Nicholls,[1] Le Nhan Pham,[1] Witold M. Bloch,[1] Lynn S. Lisboa,[1] Michael V. Perkins,[1] Christopher T. Gibson,[2] Michelle L. Coote,*[1] Zhongfan Jia,*[1] Justin M. Chalker*[1]

[1]Institute for Nanoscale Science and Technology, College of Science and Engineering, Flinders University, Bedford Park, South Australia 5042, Australia

[2]Flinders Microscopy and Microanalysis, College of Science and Engineering, Flinders University, Bedford Park, Adelaide, South Australia 5042, Australia

E-mail:
michelle.coote@flinders.edu.au
zhongfan.jia@flinders.edu.au
justin.chalker@flinders.edu.au

KEYWORDS: chemical recycling; electrochemistry; inverse vulcanization; polysulfide; sulfur

ABSTRACT: With increasing interest in high sulfur content polymers, there is a need to develop new methods for their synthesis that feature better safety and control of structure. In this report, electrochemically-initiated ring-opening polymerization of norbornene-based cyclic trisulfide monomers delivered well-defined, linear poly(trisulfides), which were solution processable. Electrochemistry provided a controlled initiation step that obviates the need for hazardous chemical initiators. The high temperatures required for inverse vulcanization are also avoided resulting in an improved safety profile. Density functional theory calculations revealed a reversible 'self-correcting' mechanism that ensures trisulfide linkages between monomer units. This control over sulfur rank is a new benchmark for high sulfur content polymers and creates opportunities to better understand the effects of sulfur rank on polymer properties. Thermogravimetric analysis coupled with mass spectrometry revealed the ability to recycle the polymer to the cyclic trisulfide monomer by thermal depolymerization. The featured poly(trisulfide) is an effective gold sorbent, with potential applications in mining and electronic waste recycling. A water-soluble poly(trisulfide) containing a carboxylic acid group was also produced and found to be effective in the binding and recovery of copper from aqueous media.

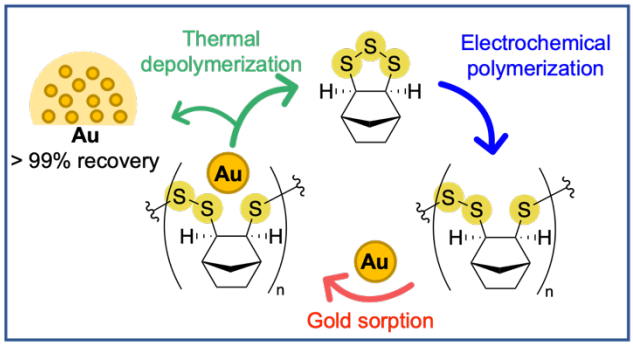

INTRODUCTION: Sulfur-rich copolymers containing S-S bonds have many useful properties such as redox activity,[1, 2] affinity for heavy metals and precious metals,[3-5] and a high refractive index of relevance to optics applications.[6, 7] Studies on the synthesis and application of polysulfide-containing polymers have been spurred by the advent of *inverse vulcanization.*[1] Introduced by Pyun and co-workers in 2013, inverse vulcanization refers to the bulk copolymerization of elemental sulfur and an organic comonomer containing one or more carbon-carbon double or triple bonds.[1] In this reaction, molten sulfur is the monomer, initiator, and solvent. At approximately 160 °C, sulfur undergoes ring-opening polymerization to form polymeric sulfur with thiyl radical end groups (Fig. 1A). These radicals can then add to the alkene or alkyne of the organic monomer, followed by further reaction with sulfur or other polysulfides in the reaction mixture. Termination, for instance by radical recombination, provides the polymer product. In contrast to classic vulcanization in which small amounts of sulfur are used to crosslink a preformed organic polymer, inverse vulcanization uses organic monomers to crosslink a polysulfide formed *in situ*.

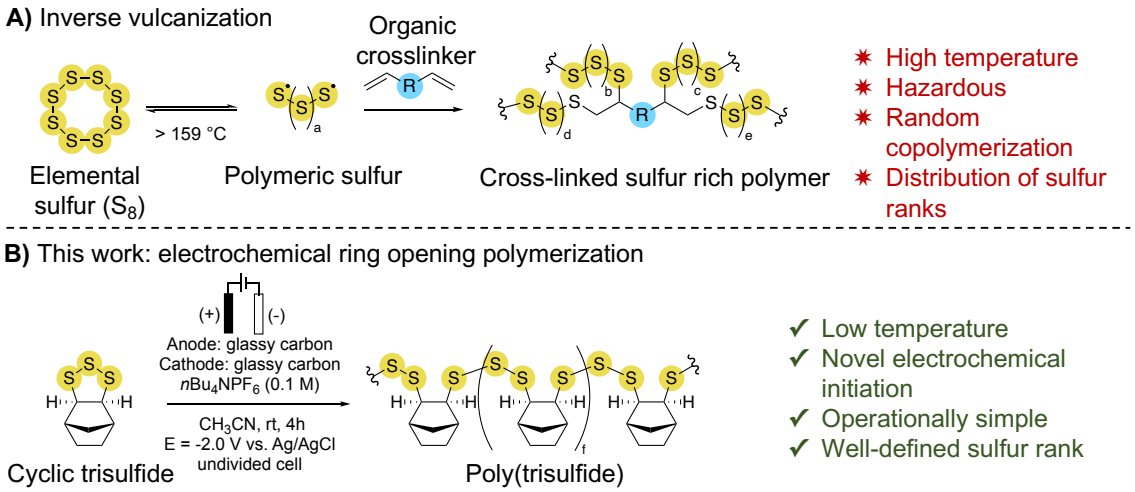

Figure 1: A) Inverse vulcanization. **B)** This work: electrochemically-induced ring-opening polymerization to provide linear polysulfides with regular sulfur rank.

Inverse vulcanization has many attractive features that have prompted a surge of activity in the field.[8-13] First, elemental sulfur is low-cost and highly abundant, with millions of tons produced in excess each year in petroleum refining,[14] and many billions of tons more in geological deposits.[15] Second, the reaction is operationally simple and typically provides polymers in short-order with high atom economy. Ready access to these polysulfides has led to diverse applications that take advantage of the useful properties of S-S bonds in these copolymers. These applications include redox active cathode materials for lithium-sulfur batteries,[1, 2] lenses and other optics equipment for infrared thermal imaging and surveillance,[7,

[16] sorbents for heavy metal remediation,[13, 17] repairable and self-healing materials,[18-20] precision fertilizers,[21-23] and recyclable machine components,[24] in addition to other applications recently reviewed.[8-12]

Despite the many useful polymers accessible by inverse vulcanization, this polymerization method does have limitations. For instance, the reaction typically requires high temperatures to form molten sulfur and induce its ring-opening polymerization (typically 160 °C or higher).[1] The high temperature may not be compatible with many organic comonomers and introduce high energy costs and safety concerns. The reaction is also frequently complicated by the immiscibility of many organic comonomers with molten sulfur, which can lead to inefficient reactions and unwanted phase separation in the product.[25] Furthermore, the exothermic nature of the inverse vulcanization can lead to runaway reactions[26] and formation of hazardous byproducts such as hydrogen sulfide[27] or malodorous thiols.[3] In terms of polymer structure, inverse vulcanization provides limited control over sulfur rank (the number of sulfur atoms between each carbon atom in the organic monomer), molecular weight, and stereochemistry of the C-S bonds.[12] Such control is important because sulfur rank influences the strength of the S-S bonds,[20, 28] which—along with molecular weight and stereochemistry—will influence the physical properties of these polymers.

Innovative solutions to some of these challenges have been reported recently. For instance, accelerators and catalysts have been reported by the Pyun and Hasell laboratories that allow inverse vulcanization to be achieved at lower temperatures, thereby suppressing byproduct formation and improving safety.[5, 29, 30] Hasell also reported alternative initiation methods that remove the need for heating including mechanochemical inverse vulcanization[31] and photoinduced inverse vulcanization.[32] Regarding control of sulfur rank and structure, Pyun and associates have recently reported alternative sulfur-derived monomers such as sulfur monochloride (S_2Cl_2) that can react with alkene-containing comonomers through a step-growth mechanism, providing polymers with disulfide linkages throughout the backbone.[33]

In this study, we report a new and complementary electrochemical polymerization method that provides poly(trisulfides) with precise control of sulfur rank (Fig. 1B). The polymerization is rapid at room temperature. The key monomers, derived from elemental sulfur and norbornene derivatives, contain a cyclic trisulfide that can be triggered to undergo ring-opening polymerization upon electrochemical reduction. Because the stereochemistry of the C-S bond is fixed before polymerization, this aspect of the final polymer structure is also controlled. The process is operationally simple and does not require an inert atmosphere, which is more robust than related anionic ring-opening polymerizations.[34] Running at ambient temperature, the formation of hazardous byproducts such as hydrogen sulfide is completely avoided. The polymerization was also investigated computationally, revealing an intriguing self-correcting mechanism that ensures selective formation of trisulfide links in the repeating unit, rather than

disulfide or tetrasulfide links that could conceivably form through alternative, but kinetically unfavored, pathways. With reliable access to poly(trisulfide) materials, several applications were explored including high-yielding depolymerization for monomer recycling, gold and copper sorption and recovery, and covalent modification post-polymerization.

RESULTS AND DISCUSSION:

Monomer synthesis

Elemental sulfur, in the presence of a nickel(II) catalyst, can add across the strained alkene of norbornene and its derivatives, providing cyclic polysulfide products in which the vicinal C-S bonds have a *cis* stereochemical relationship (S2-S18).[35] It was envisioned that these well-defined polysulfides would provide a good testing ground for electrochemically-induced ring-opening polymerization as an alternative to inverse vulcanization in accessing polysulfide polymers. Trisulfide **1**, as a monomer with high symmetry, was anticipated to simplify spectroscopic analysis of the reaction and products. Monomer **1** and polymers derived from **1** are also high in sulfur content (50 wt% sulfur), which is comparable to many polymers made by inverse vulcanization.[10] Monomers **3** and **4** were made to assess functional group tolerance and also provide a handle for post-polymerization modification. Trisulfides **1**, **3** and **4** were therefore prepared by adapting the method previously reported by Poulain (Fig. 2).[35] Pentasulfide monomer **2** was isolated as a minor product in the preparation of trisulfide monomer **1**. The cyclic sulfides were purified by vacuum distillation or flash column chromatography providing monomer **1** as an oil and monomers **2**-**4** as crystalline solids. All monomers were characterized by NMR, IR, and Raman spectroscopy, mass spectrometry, and elemental analysis (S6-S18). The structures of monomers **2**-**4** were determined unambiguously by single crystal X-ray crystallography (Fig. 2 and S19-S20). In all cases, the polysulfide monomers were isolated as the *exo* isomers in which the two C-S bonds have a *cis* relationship on the same face as the bridgehead methylene group (Fig. 2 and S20).

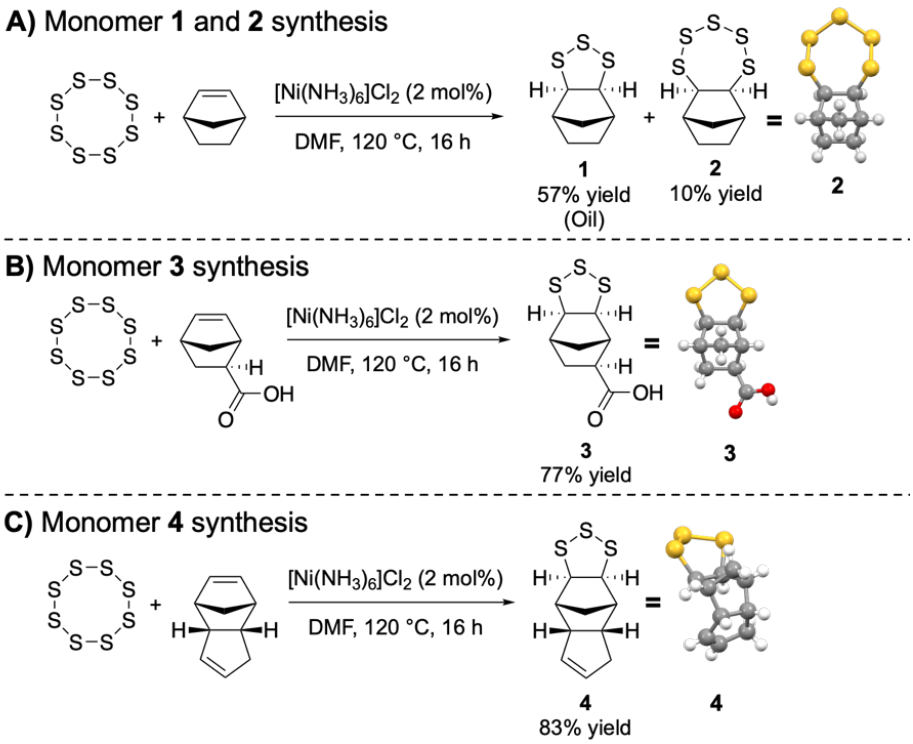

Figure 2: A) Reaction of sulfur and norbornene to form monomer **1** and **2**. **B)** Synthesis of monomer **3**, containing a carboxylic acid. **C)** Reaction of sulfur and dicyclopentadiene to form monomer **4**. Single crystal X-ray structures of monomers **2**-**4** are shown.

Monomer redox activity

Cyclic voltammetry was used to assess the electrochemical redox behavior of monomers **1**-**4** (S23-S25). Cyclic voltammetry of each monomer was measured between -3.0 and +1.5 V versus Fc/Fc^+ in a 0.1 M nBu$_4$NPF$_6$ acetonitrile solution (Fig. 3A). This electrolyte and solvent were selected as they have stability across the potential range of interest, and more efficient reaction of the monomer was observed in this solvent than was observed for other solvents such as DMF, THF, and dichloromethane (S26-S27). Trisulfide monomers **1**, **3** and **4** exhibited two irreversible redox peaks, a cathodic peak between -2.5 and -2.2 V versus Fc/Fc^+, and an anodic peak between -1.0 and -1.4 V versus Fc/Fc^+ (Fig. 3A). The cyclic voltammogram of pentasulfide monomer **2** presents additional redox features at -1.6 and -0.8 V versus Fc/Fc^+ (Fig. 3A). These lower redox potentials are likely derived from the different redox activity of the five-membered sulfur ring in monomer **2** compared to the trisulfide structure of the other monomers. Interestingly, the cyclic voltammograms of both monomer **1** and **2** contain cathodic peaks at -2.2 V versus Fc/Fc^+. Investigating this result further by ^{1}H NMR spectroscopy revealed that electrochemical reduction of pentasulfide monomer **2** resulted in its partial desulfurization to form monomer **1** in addition to other products (S35-S36). Due to this complex reactivity profile, monomer **2** was not studied further in polymerization tests and focus was placed on trisulfide monomers **1**, **3** and **4**.

The irreversible nature of the redox events for monomer **1** was corroborated across a range of scan rates between 50 and 1000 mV/s (S24). The irreversibility suggests a fast chemical reaction occurs immediately following oxidation or reduction. In preliminary investigations, applying a positive potential did not generate polymer from the trisulfide monomers, so this mode of initiation was not pursued further. Instead, electrochemical reduction of cyclic trisulfide monomers **1**, **3**, and **4** was targeted to initiate ring-opening polymerization by way of a putative radical anion intermediate (see polymerization studies and mechanistic discussion below).

Density functional theory (DFT) calculations were performed to investigate the reduction potential required for each monomer and compare it to those obtained experimentally. The calculated values closely matched the experimentally observed reduction potential of trisulfide monomers **1**, **3**, and **4** (Fig. 3B). These comparisons provided confidence in the accuracy of the calculations and corroborated the hypothesis that the initial step in the electrochemical reaction is the addition of an electron to the trisulfide monomer (*vide infra*). For cyclic pentasulfide monomer **2**, the electrochemical reduction was more complicated, as mentioned previously. During this process, the pentasulfide was reduced (-1.6 V versus Fc/Fc^+) and converted into cyclic trisulfide monomer **1**. ^1H NMR spectroscopy confirmed this electrochemically-initiated ring contraction (S35-S36). Therefore, the peak at -2.2 V versus Fc/Fc^+ in the cyclic voltammogram of monomer **2** is actually due to reduction of monomer **1** formed during the measurement.

A) Cyclic voltammetry

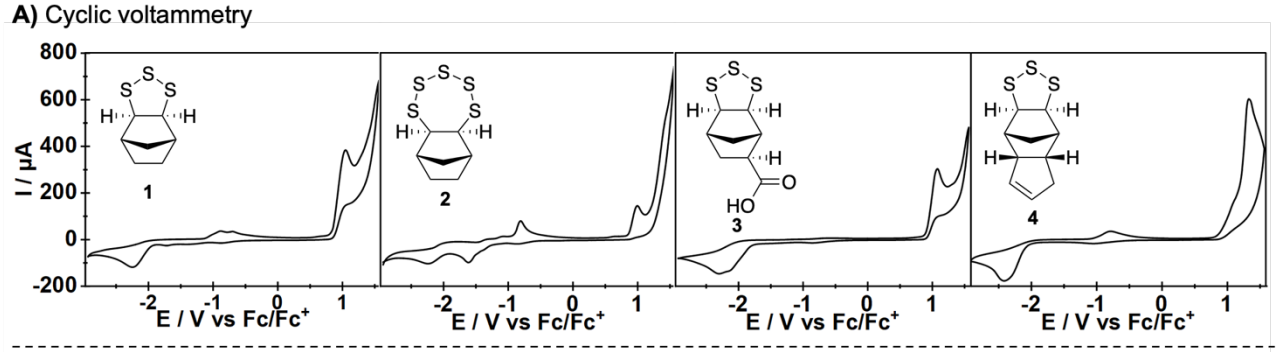

B) Monomer reduction potential

	1	2	3	4
Calculated vs Fc/Fc^+	-2.29 V	-2.05 V	-2.24 V	-2.28 V
Measured vs Fc/Fc^+	-2.22 V	-2.21 V, -1.60 V	-2.27 V	-2.30 V

Figure 3: A) Cyclic voltammograms of cyclic sulfide monomers (5 mM) were measured in a potential window of -3.0 and +1.5 V versus Fc/Fc^+ at 100 mV/s showing the third cycle. The supporting electrolyte was a solution of 0.1 M nBu$_4$NPF$_6$ in acetonitrile (10 mL). **B)** Conditional formal reduction potentials calculated in acetonitrile (V versus Fc/Fc^+) at the wB97XD/def2TZVPD//wB97XD/6-31+G(d,p) level of theory using the SMD solvent model, and comparison to the experimentally measured values.

Following the cyclic voltammetry measurements, chronoamperometry experiments were then conducted by applying a constant potential of -2 and +2 V versus Ag/AgCl to divided cells containing monomer **1** (S25). Current was observed when a negative potential was applied, and no current was observed when a positive potential was applied. Additionally, a product precipitated in the cathodic chamber in these experiments. This product was later identified as **poly-1**, providing motivation to investigate and optimize the polymerization of the trisulfide monomers under a reductive potential.

Electrochemical polymerization

Guided by cyclic voltammetry, preliminary computational studies, and the divided cell experiment discussed previously, we arrived at a working hypothesis that a ring-opening reaction of the monomers is induced by cathodic reduction of the monomer. To study this process in greater detail, we targeted the ring-opening polymerization of monomer **4** for its easily identifiable ^{1}H NMR signals that did not overlap with the electrolyte during analysis of crude reaction mixtures. Monomer **4** (0.04 M) was dissolved in a solution of acetonitrile (15 mL, 0.1 M nBu$_4$NPF$_6$) in an ElectraSyn® cell containing two glassy carbon electrodes and a Ag/AgCl reference electrode. Glassy carbon was chosen as the working and counter electrode material due to its low cost, wide potential range, and stability under the reaction conditions. While stirring, a constant potential of -2.0 V versus Ag/AgCl was applied to the cell resulting in the immediate formation of precipitate (Fig. 4B). Over 4 hours the amount of precipitate in the cell increased and became darker in color. The precipitate was collected and purified by successive dissolution in chloroform and precipitation with acetonitrile to isolate the final product for further characterization (S26-S47). The product was soluble in both chloroform and THF, which allowed analysis by ^{1}H NMR spectroscopy and gel permeation chromatography (GPC), respectively. The ^{1}H NMR spectrum of the purified product showed broad peaks consistent with a polymer structure (Fig. 4C). Integration of the alkene signals revealed no reaction occurred at this functional group, which is evidence for chemoselectivity in the ring-opening polymerization. GPC data indicated a weight average molecular weight (M_w) of 3900 g/mol and a polydispersity (Đ) of 1.91 when calibrated against polystyrene standards (Fig. 4D). FTIR spectra of the polymer showed broadened peaks compared to monomer **4** (Fig. 4E) and Raman spectroscopy revealed fluorescence when analyzed with either a 532 nm laser (Fig. 4F) or a 785 nm laser (S45). This fluorescence is consistent with previous reports of dicyclopentadiene-sulfur copolymers, which makes it difficult to draw conclusions from the Raman spectra with regards to sulfur rank.[36] With that said, subtle differences in the S-S signals of the Raman spectra could be resolved for linear disulfide and trisulfide small molecule models and the cyclic trisulfide and pentasulfide monomers (S18). This important series of control experiments indicate the possibility for

distinguishing sulfur ranks by Raman spectroscopy, in line with a recent report by Dodd, Hasell and co-workers.[36] Furthermore, reduction of the polymer with $LiAlH_4$ produced dithiol **5**, corroborating the proposed polymer structure (Fig. 4G).

Several important conclusions could be drawn from this initial study of the polymerization of monomer **4**. First, cathodic reduction of monomer **4** rapidly produced polymer, as evidenced by ^{1}H NMR spectroscopy, GPC, and Raman spectroscopy. Second, the polymer was soluble in many organic solvents—an advantageous property for polymer processing. Third, the reaction was chemoselective: no reaction occurred at the alkene and polymerization was therefore due to a ring-opening reaction of the trisulfide functional groups.

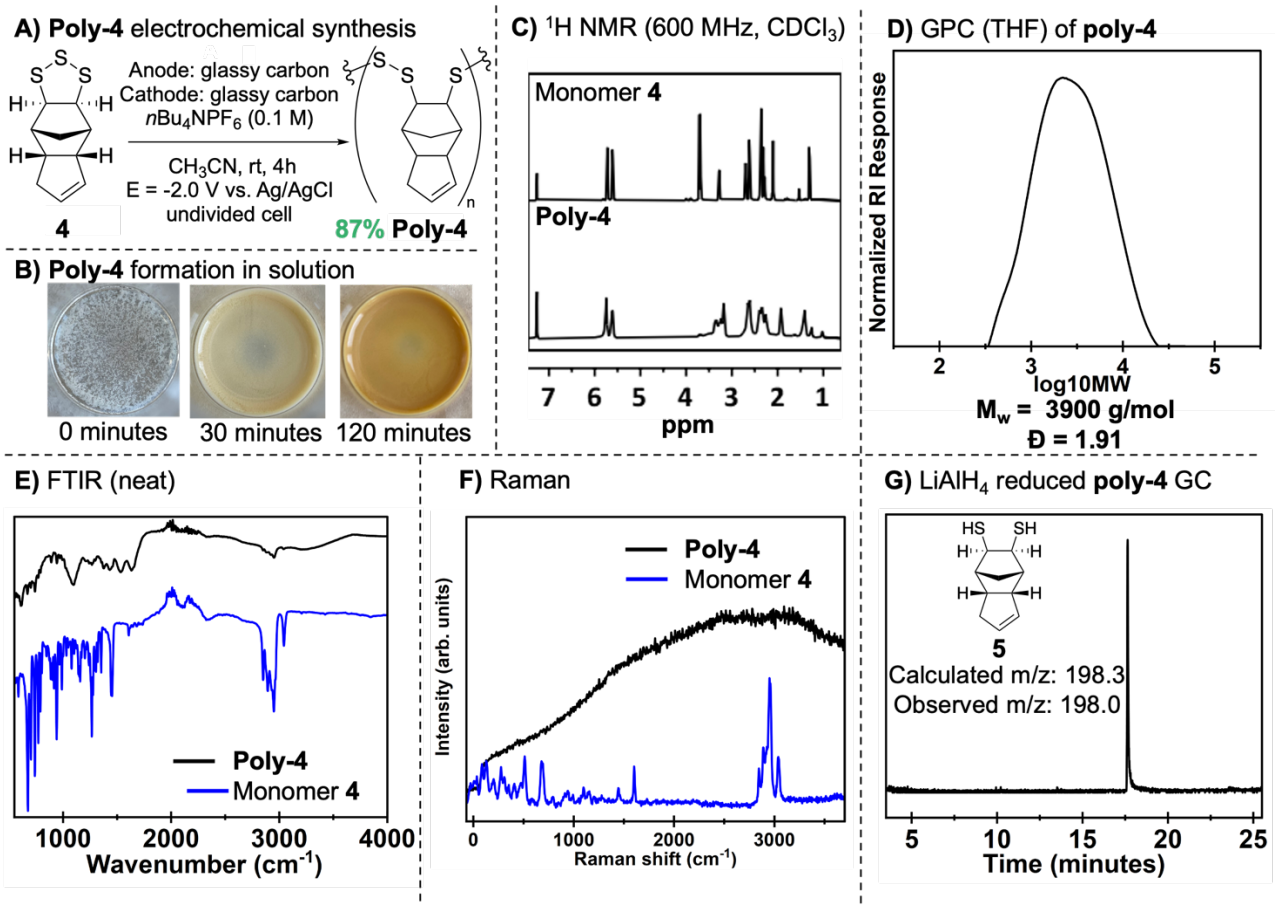

Figure 4: A) Conditions for electrochemical polymerization of monomer **4**. **B) Poly-4** precipitated from the reaction mixture over the course of the reaction. **C)** The ^{1}H NMR spectrum of **poly-4** showed broad signals compared to monomer **4**, consistent with the formation of a polymer structure. The alkene signals between δ = 5.6-5.8 ppm indicated that no reaction occurred at this functional group. **D)** GPC trace of **poly-4**. The M_w was 3900 g/mol and the Đ was 1.91. **E)** Infrared spectra of monomer **4** and **poly-4**. **F)** Raman spectra of monomer **4** and **poly-4** using a 532 nm laser. **G)** Reduction of **poly-4** with $LiAlH_4$ resulted in the formation of expected dithiol **5**. The gas chromatogram of the dithiol is shown, along with mass spectrometric

data. This reaction was consistent with the polysulfide structure of **poly-4** and confirmed the alkene of monomer **4** did not react in the polymerization.

Different polymerization conditions were evaluated next, focusing on monomer conversion, polymer yield, M_w and Đ (Table 1). Each reaction was run in a 20 mL undivided ElectraSyn® cell containing monomer **4** (0.04 M) dissolved in acetonitrile (15 mL, 0.1 M nBu$_4$NPF$_6$). The polymer product was isolated and analyzed by GPC. The integrations of the resonances in the ^{1}H NMR spectrum of monomer **4** and the electrolyte (nBu$_4$NPF$_6$) were compared to determine monomer conversion of crude reaction mixtures. Entry 1 was run under a constant potential of -2.0 V versus Ag/AgCl in a cell containing two glassy carbon electrodes and an Ag/AgCl reference electrode. After 30 minutes, monomer conversion was calculated to be 66%, while isolated polymer yield was 32%. This indicated the method of purification by successive precipitation excluded lower molecular weight polymers which were soluble in acetonitrile. The isolated product had a M_w of 3370 g/mol and a Đ of 2.14.

The lower cost of graphite compared to glassy carbon electrodes motivated us to test them in the ring-opening polymerization reaction. Graphite electrodes (entry 2) performed similarly to glassy carbon electrodes with 66% conversion (entry 1). However, electrode degradation was observed during the reaction which could contaminate the polymer product. Therefore, boron-doped diamond electrodes (BDD) were tested next because they are known to exhibit superior electrochemical stability (entry 3).[37] Using BDD electrodes, the monomer conversion and polymer yield were increased slightly to 73% and 45%, respectively. GPC analysis revealed the polymer produced using BDD electrodes had a lower M_w when compared to glassy carbon electrodes. However, due to the high cost of BDD electrodes, glassy carbon electrodes were used for subsequent reactions.

The effect of different potentials on the system was investigated next. At -1.6 V versus Ag/AgCl (entry 4) a decrease in monomer conversion (44%) and polymer yield (25%) was observed. This result was anticipated because less efficient reduction of the monomer was expected at this potential. Interestingly, a larger M_w of 6030 g/mol and a broader Đ were obtained at this potential in comparison to the standard reaction at -2.0 V versus Ag/AgCl. Relatedly, when the potential was decreased to -2.4 V versus Ag/AgCl (entry 5) there was an increase in monomer conversion (78%) and a decrease in polymer yield (28%). At this potential, a smaller M_w of 2760 g/mol was obtained. Together, these results suggest that changing the reactor potentials can be used for some control over the molecular weight of the polymer.

Next, the reaction was run under an inert atmosphere of argon (entry 6). All glassware and reagents were also rigorously dried. Little difference in the reaction outcome was observed when run in either open air or argon. This was an important and surprising finding indicating that the electrochemical polymerization does not require an inert atmosphere, which simplifies

the process. In contrast, anionic polymerization of the trisulfide monomers is highly sensitive to moisture and oxygen, and requires tedious preparation of initiators.[34] Notably, our attempted nucleophile-initiated anionic polymerization of the trisulfide monomers was unsuccessful and repeatedly resulted in recovered monomer (S21).

Constant current reactions are commonly used in electrochemical synthesis as they can be run without the need for cyclic voltammetry studies. Therefore, for entry 7 the polymerization was carried out at a constant current of 10 mA in a two-electrode cell. This resulted in a 68% conversion of monomer and a 12% polymer yield with a Đ of 9.98. Low polymer yield and broad Đ were expected for the constant current reaction because it did not target the precise reduction potential of the monomer and can therefore result in inconsistent monomer consumption and other side reactions. The disparity between monomer conversion and polymer yield suggests that the formation of lower molecular weight oligomers and polymers are excluded by the isolation procedure. This was also consistent with the broad Đ inferred from GPC.

Finally, the reaction time was increased to 60 minutes (entry 8), 120 minutes (entry 9) and 240 minutes (entry 10) to improve polymer yield. Entry 10 resulted in 99% monomer conversion and a high polymer yield of 87%. M_w and Đ show consistency across all three reactions under the same conditions. We propose this uniformity is the result of polymer precipitation due to its insolubility at those molecular weights.

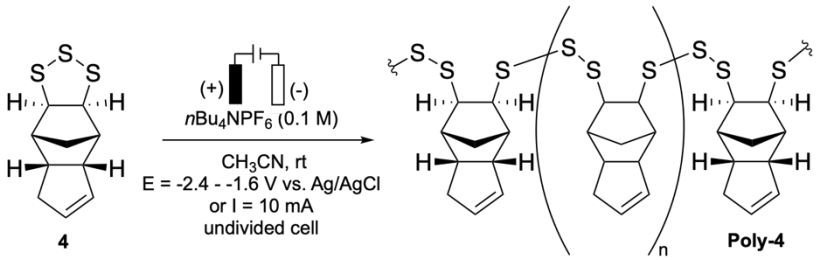

Entry	Electrode material (anode + cathode)	Reaction time (min)	E or I	e⁻ equiv. (F/mol)	Conversion (%)	Yield (%)	M_W (g/mol)	Đ
1	Glassy carbon	30	-2.0 V	1.63	66	32	3370	2.14
2	Graphite	30	-2.0 V	1.16	66	44	3960	4.20
3	Boron doped diamond	30	-2.0 V	1.82	73	45	3350	4.12
4	Glassy carbon	30	-1.6 V	0.71	44	25	6030	4.47
5	Glassy carbon	30	-2.4 V	3.12	78	28	2760	3.20
6[a]	Glassy carbon	30	-2.0 V	1.76	62	34	3110	3.88
7	Glassy carbon	30	10 mA	0.62	68	12	3990	9.98
8	Glassy carbon	60	-2.0 V	1.59	66	24	3920	2.01
9	Glassy carbon	120	-2.0 V	5.26	99	74	3890	2.01
10	**Glassy carbon**	**240**	**-2.0 V**	**7.05**	**99**	**87**	**3900**	**1.91**

[a] Conducted under argon atmosphere

Table 1: Optimization of reaction conditions for polymerization of monomer **4**

Polymerization kinetics

Polymerization kinetics of monomer **4** were studied using conditions in Table 1, entry 9. Aliquots were taken from the polymerization reaction over 2 hours and analyzed by GPC (Fig. 5) and ^{1}H NMR spectroscopy. The conversion of monomer **4** was assessed based on integration of the resonances in the ^{1}H NMR spectrum of monomer **4** compared to that of the electrolyte (nBu$_4$NPF$_6$) (S48-S49). Pseudo first-order behavior was observed during this polymerization indicating a constant concentration of reduced monomer and rapid polymerization (Fig. 5A).

Over the 2 hours, a maximum M_w of 4950 g/mol was observed (Fig. 5C). The limited molecular weight of the polymer is likely a result of polymer precipitation at that chain length with these reaction conditions. While the molecular weights obtained with this method are relatively low, this precipitation polymerization does provide a self-protection mechanism against reductive degradation of the polymer. This feature contrasts to homogenous chemical initiation methods such as photoredox catalysis or chemical reduction which could potentially react with and reduce the polymer, rather than just the monomer. Finally, it was observed that the distribution of polymer molecular weight decreased over the reaction, resulting in a more uniform Đ (Fig. 5D). This is likely a result of lower molecular weight oligomers converting to longer-chain polymers and precipitating from solution.

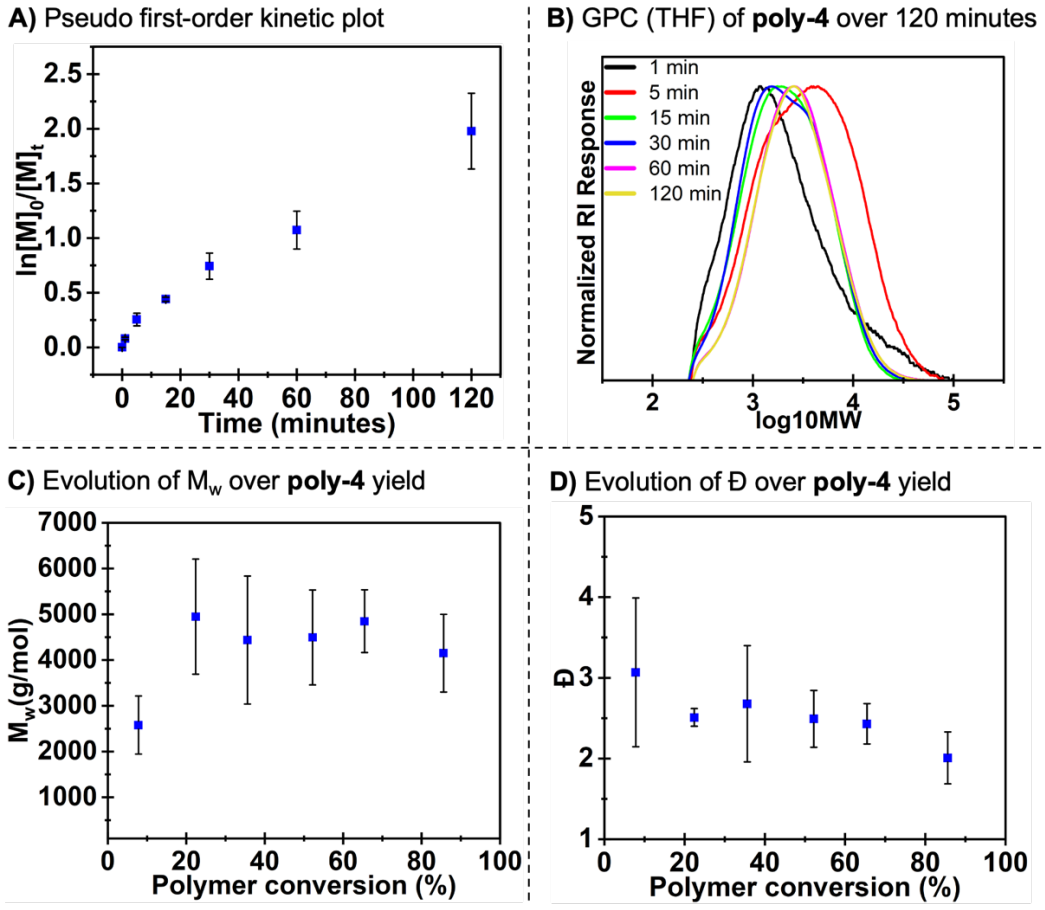

Figure 5: A) Pseudo first-order kinetic plot of monomer **4** consumption where $\ln[M]_0/[M]_t) = k_1t$ ([M] = monomer **4** concentration (M), t = time (minutes), k = first-order rate constant

(M/minute). **B)** GPC (THF) of **poly-4** over 120 minutes of reaction time. **C)** Evolution of the M_w of **poly-4** against **poly-4** conversion. **D)** Evolution of Đ of **poly-4** against **poly-4** conversion. All data was collected in triplicate.

Next, the optimized conditions (Table 1, entry 10) for the synthesis of **poly-4** were applied to monomers **1** and **3**. Specifically, the monomers were dissolved in a solution of acetonitrile so that the initial monomer concentration was 0.04 M. An undivided cell was used in the ElectraSyn® reactor equipped with two glassy carbon electrodes and an Ag/AgCl reference electrode. The supporting electrolyte was nBu$_4$NPF$_6$ (0.1 M in acetonitrile, 15 mL) and the polymerizations were initiated by applying a constant potential of -2.0 V versus Ag/AgCl. The reactions were run for 4 hours at room temperature with stirring. As in the synthesis of **poly-4**, **poly-1** and **poly-3** also precipitated during the reaction. **Poly-1** was isolated in 83% yield, with GPC analysis indicating a M_w of 6580 g/mol and a Đ of 3.08 (Fig. 6).

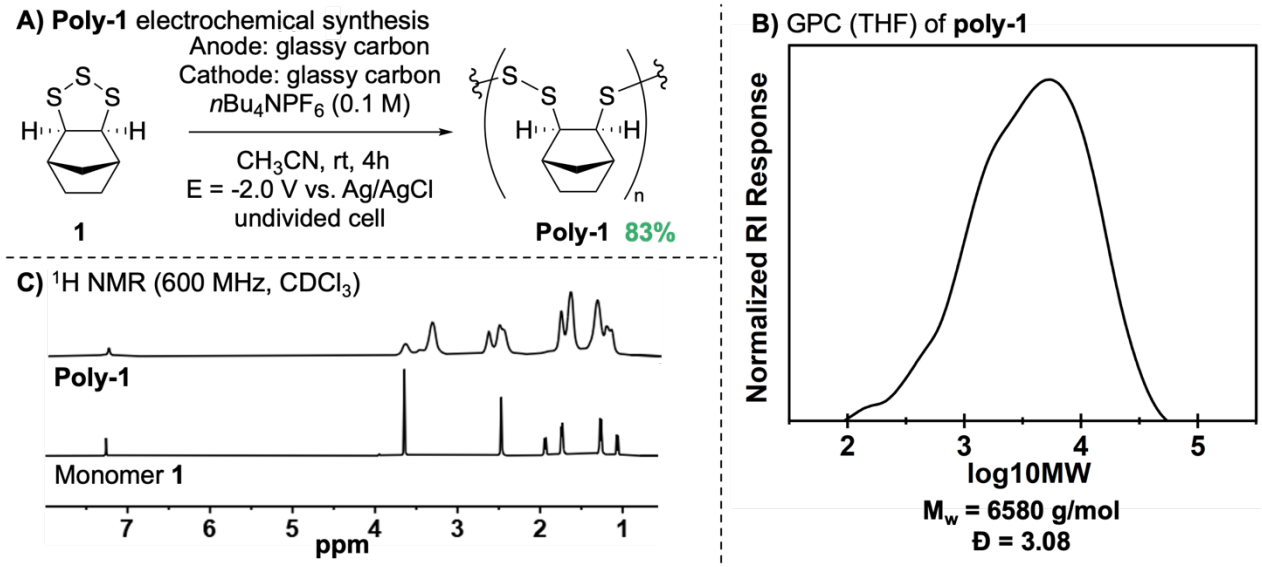

Figure 6: A) Conditions for electrochemical polymerization of monomer **1**. **B)** GPC trace of **poly-1**. The M_w was 6580 g/mol and the Đ was 3.08. **C)** ^{1}H NMR spectrum of **poly-1** has broad signals in comparison to monomer **1**, consistent with the formation of a polymer structure.

The formation of **poly-3** is also notable in that the carboxylic acid functionality was tolerated (Fig. 7). Evidence for the stability of the carboxylic acid group under these conditions can be observed by the characteristic carbonyl stretch present in the infrared spectrum of **poly-3** (Fig. 7B). **Poly-3** was isolated in a synthetically useful yield of 59%. Aqueous GPC analysis of **poly-3** combined equimolar quantities of NaOH per carboxylic acid indicated a M_w of 8530 g/mol and a Đ of 1.31. **Poly-3** was soluble in water when the carboxylic acid groups were deprotonated by equimolar quantities of NaOH (Fig. 7C). Successful preparation of **poly-3** represents a

significant advance in producing water-soluble polysulfides, few of which have been made by inverse vulcanization.[38] Aqueous solubility of sulfur rich polymers may provide benefits in sorption of valuable metals in aqueous media, as previously shown by Jenkins and co-workers,[38] so this behavior for **poly-3** was investigated further (*vide infra*).

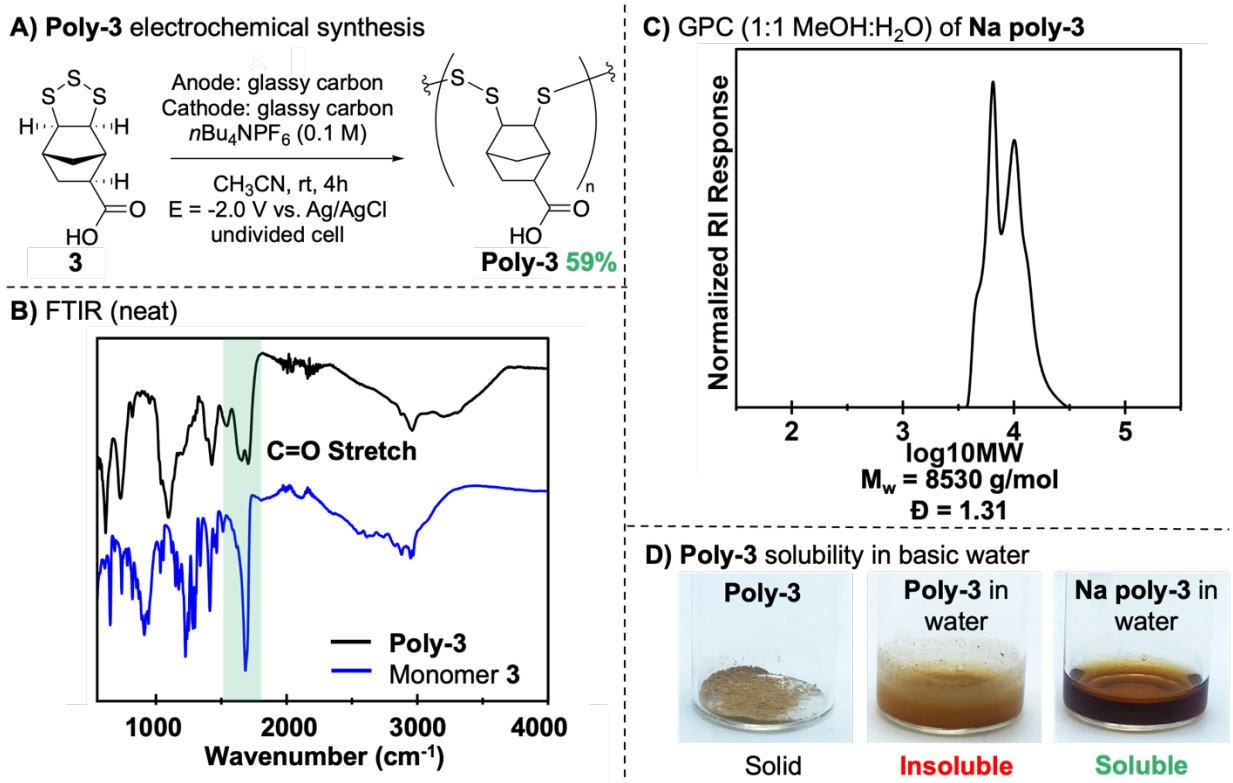

Figure 7: A) Conditions for electrochemical polymerization of monomer **3**. **B)** Infrared spectra of monomer **3** and **poly-3**. **C)** GPC trace of **Na poly-3**. The M_w was 8630 g/mol and the Đ was 1.31. **D) Poly-3** is not water-soluble, but soluble in water with one mol equivalent of NaOH per carboxylic acid.

Polymerization mechanism

To understand the mechanism in more detail, polymerization of the simplest monomer (**1**) was investigated using DFT calculations (Fig. 8 and S52-S78 for additional details of the method and data). The initiation step was studied first (Fig. 8A). As discussed previously, the calculated reduction potential for monomer **1** (-2.29 V versus Fc/Fc^+) was consistent with the experimentally observed value (-2.22 V versus Fc/Fc^+) (Fig. 3). Upon reduction and formation of radical anion **6**, the monomer does not spontaneously ring-open, but the Gibbs free energy barrier for it to do so is only 18.9 kJ/mol, which is considerably less than the corresponding 165.0 kJ/mol barrier for ring-opening of the neutral (unreduced) monomer **1**. In Figure 6A, the ring-opened, reduced species **8** is drawn with a formal negative charge on the terminal monosulfide and a formal radical on the terminal disulfide; this depiction best reflects the

computed spin- and charge-density distribution, though we note that both sulfur end groups of **8** have some anionic and some radical character. Either of these sulfur centers of intermediate **8** may in principle attack the neutral monomer to start the polymerization process, with attack by the terminal monosulfide best represented as an anionic ring-opening process, and attack by the terminal disulfide best represented as a radical process (Fig. 8B). Of both pathways, attack by the monosulfide anion was found to be considerably more kinetically favorable than radical attack by the disulfide terminus, so the latter can be ruled out. The monosulfide anion can then attack the terminal sulfur in the monomer to form a disulfide linkage and a new terminal disulfide anion (Fig. 8B, intermediate **9**). Alternatively, the central sulfur atom can be attacked to form a trisulfide linkage and a terminal monosulfide anion (Fig 8B, intermediate **10**). Based on the calculations, both reactions are likely to occur, with an approximate 8:1 preference for the latter. As both products are thus likely to be produced, they were both considered for the next propagation step.

Figure 8B shows the barriers and Gibbs free energies for the first and second propagation steps. Four reactions were considered, corresponding to the two most likely products of the first propagation step attacking either the terminal or central sulfur of the trisulfide monomer. As in the case of the first propagation step in which the reaction of the disulfide radical was not favored, the reactions of the disulfide anion are also strongly kinetically and thermodynamically disfavored. In other words, the reactions of intermediates **9** or **11** with monomer **1** have such a high barrier that these reactions are not expected to compete. The monosulfide anion in **10**, on the other hand, can attack either the central sulfur atom on the trisulfide monomer to form a new terminal monosulfide anion (**12**), or the terminal sulfur of the trisulfide monomer to form a new disulfide linkage (**11**). Barriers for both reactions are similar, with the rate of attack at the central sulfur atom having a 3:1 kinetic preference. While not kinetically preferred, attack at the terminal sulfur, forming a terminal disulfide anion, has a significant (28 kJ/mol) thermodynamic preference. However, based on the calculations in Figure 8B, the disulfide products (such as **9** and **11**) of this latter process are predicted to be unreactive to further propagation. Therefore, only addition of a monosulfide anion end group to the central sulfur atom of the trisulfide monomer would lead to further chain growth. As a result, the predominant repeat unit is predicted to be a trisulfide linkage. It should be noted that the propagation reactions are reversible at room temperature, which may limit the attainable molecular weight of the polymer. With that said, the reversibility allows for a "self-correction" mechanism that can convert disulfide products back to the pathway that provides a polymer with trisulfides in the repeating unit. The termination mechanism was not studied computationally, but based on our experimental observations we propose that the termination event is aided by precipitation of the polymer, which occurs during the polymerization process at the measured molecular weights.

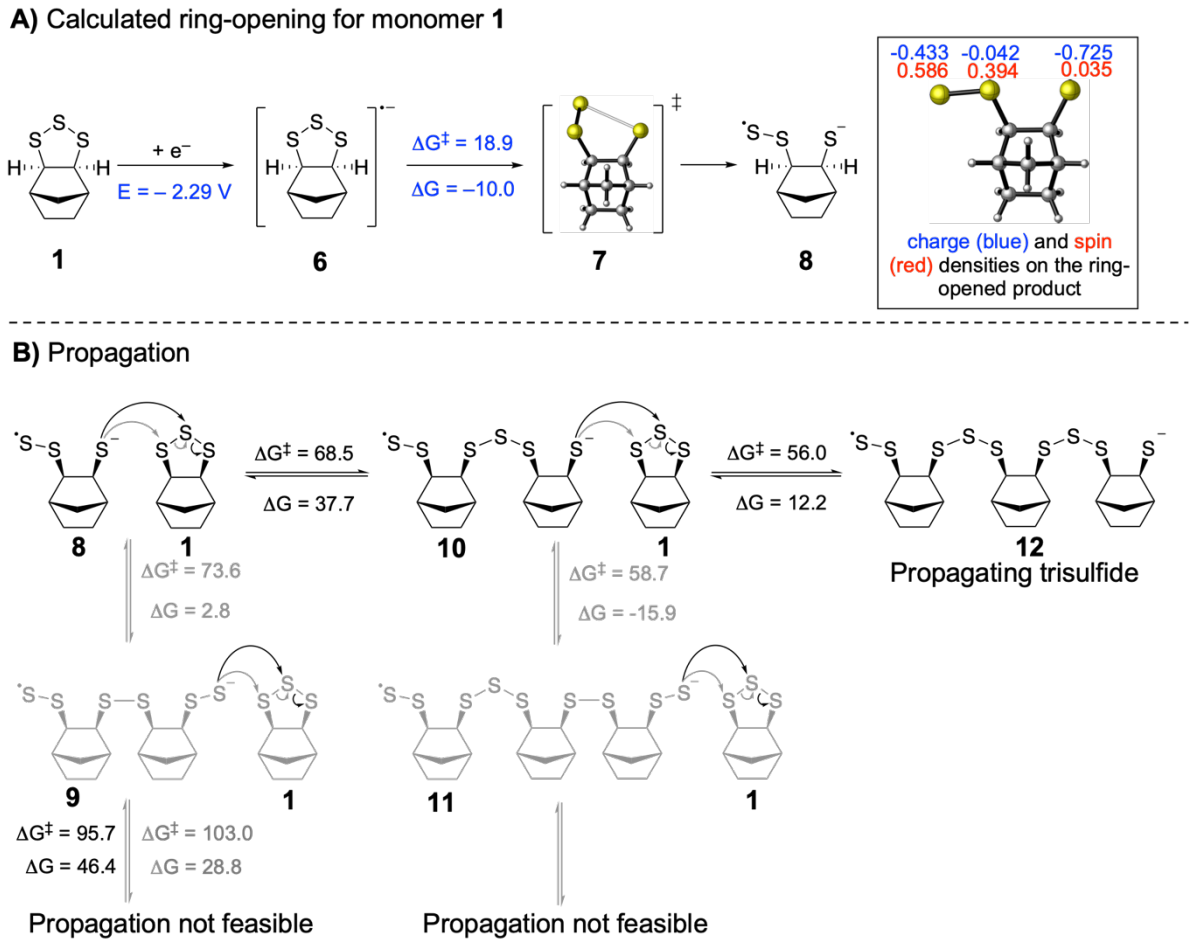

Figure 8: Theoretical investigation of the polymerization mechanism. DFT calculations were performed at the wB97XD/def2TZVPD//wB97XD/6-31+G(d,p) level of theory using the SMD solvent model. **A)** Initiation occurs by ring opening of a radical anion formed by electrochemical reduction of monomer **1**. Gibbs free energy barriers and reaction energies (298 K, kJ/mol) for the ring opening of the reduced norbornene trisulfide monomer in acetonitrile. The inset shows the charge (blue) and spin (red) densities on the sulfur atoms in the ring-opened, reduced species. **B)** Calculated initiation pathways indicate propagation is kinetically favored by ring-opening polymerization due to a terminal monosulfide anion attacking the central sulfur atom of monomer **1**. Gibbs free energy barriers and reaction energies (298 K, kJ/mol) in acetonitrile are shown for possible propagation pathways. Products **9** and **11** contain disulfide linkages, but do not propagate due to high reaction barriers in the reaction with monomer **1**. The reversibility of these reactions allows for "self-correction" and formation of the trisulfide linkage in the propagating species (**10** and **12**).

Thermal depolymerization

Polymer waste is increasingly problematic for environmental and human health.[39] Recycling efforts are critical in addressing this issue, but most thermoplastic polymers are mechanically recycled, which results in structural degradation and downcycling to lower-value

products.[40, 41] Chemical recycling, in contrast, is an increasingly attractive process in which polymers are converted back to their original monomer.[41, 42] Examples include solvolysis of polyesters and polycarbonates,[43] pyrolytic or catalytic depolymerization of polyolefins,[44] and depolymerization of polymers with dynamic covalent bonds.[45] While encouraging progress has been made on this front, these methods are often hampered by the requirement for solvent or exogenous reagents, high energy consumption, or polymer degradation to unwanted byproducts.[45] Here, the thermal depolymerization of **poly-1** was investigated with an aim to introduce a new example to the growing list of chemically recyclable materials (Fig. 9). It was anticipated that simply heating this poly(trisulfide) could induce homolytic S-S cleavage in the trisulfide backbone, followed by back-biting to regenerate monomer **1**. Due to the volatility of monomer **1**, direct distillation was investigated as a simple method for purification and recovery of recycled monomer **1**. Importantly, this depolymerization strategy does not require solvent or exogenous reagents, thereby relying only on the innate reactivity of the polymer.

First, the thermal stability of **poly-1** was studied using thermogravimetric analysis coupled with gas chromatography-mass spectrometry (TGA-GC-MS) (Fig. 9A and S79-S80). The TGA indicated the onset of mass loss above 140 ºC, with quantitative mass loss after heating to temperatures >210 ºC. The GC-MS data of the volatilized material was remarkably clean: between 140 ºC and 160 ºC only a single peak was observed, with a mass matching that of monomer **1** (Fig. 9B). Traces of other products were detected at temperatures exceeding 170 ºC, so preparative chemical recycling was tested next at 150 ºC. In the event, **poly-1** was heated at 150 ºC under reduced pressure (1 mbar) in a short-path distillation apparatus. After 4 hours, depolymerization was complete and the monomer distilled and isolated as a yellow oil. ^{1}H NMR spectroscopy analysis confirmed the high purity of the regenerated monomer, which was isolated in 72% yield (Fig. 9D and S81-S84). The high yield, recycled monomer purity, and simplicity of the depolymerization compares favorably to many other depolymerization reactions.[42-45]

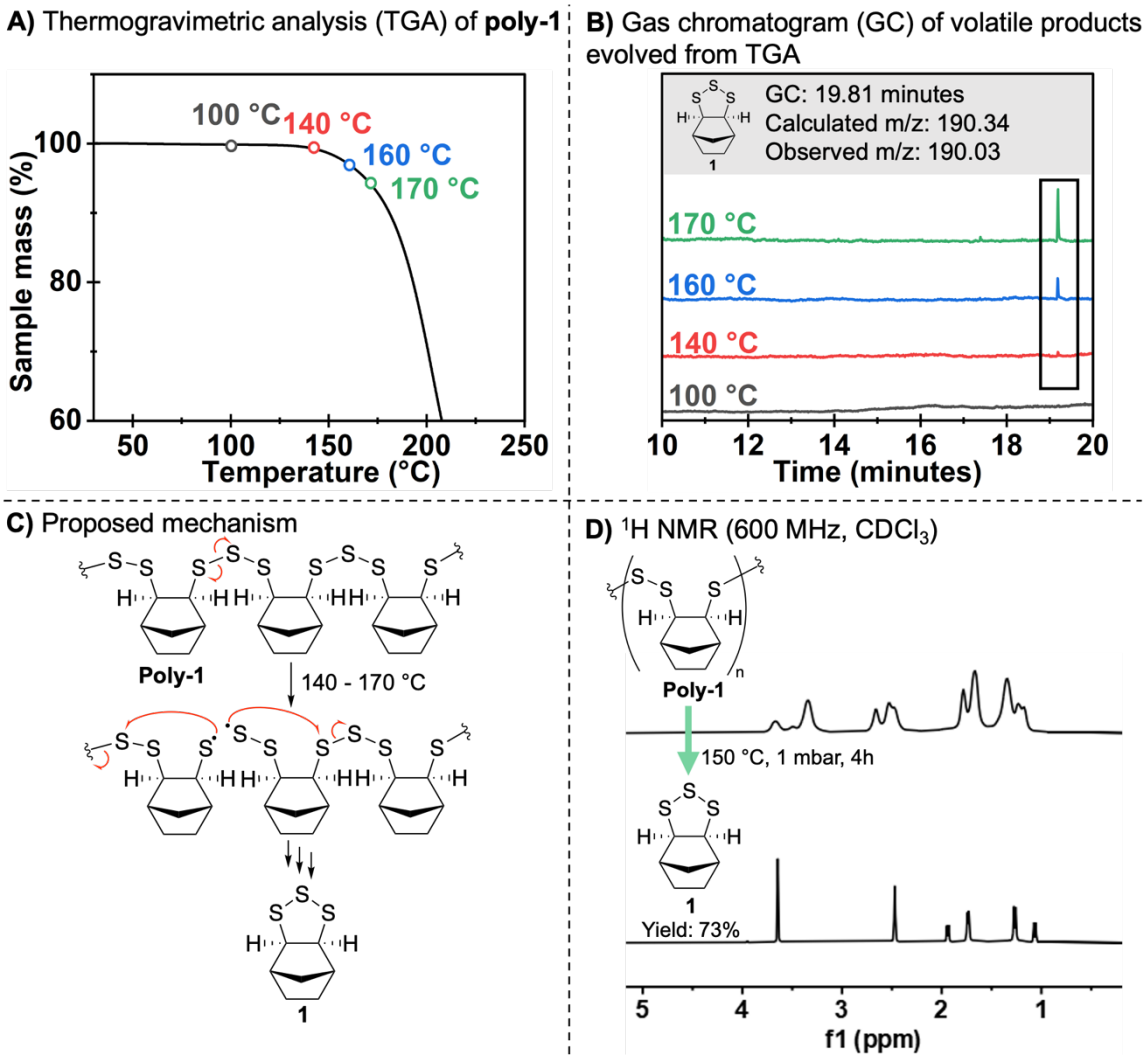

Figure 9: A) TGA indicating onset of mass loss from a sample of **poly-1** above 140 °C. **B)** GC and MS data of off-gas generated in TGA analysis indicating a single product (monomer **1**) was formed when **poly-1** is heated between 140 °C and 170 °C. **C)** Proposed depolymerization mechanism involving homolytic cleavage of S-S bonds of **poly-1**, followed by backbiting to reform monomer **1**. **D)** Preparative depolymerization in which the depolymerization of **poly-1** was done under reduced pressure to distill and recover regenerated monomer **1** in a 73% isolated yield. ^{1}H NMR spectrum analysis confirmed the formation of **1** in high purity.

Gold sorption and recovery

Safe and sustainable gold recovery is an important concern in mining[46] and electronic waste recycling.[47] Polysulfides made by inverse vulcanization and related processes are promising in this regard,[5, 48] but methods to separate the polymer and gold are limited and typically require pyrolysis or chemical degradation of the polymer.[48] Given the efficient thermal depolymerisation of **poly-1**, it was hypothesised that after **poly-1** bound to gold salts, could be thermally depolymerised and separated from the precious metal.

To test this design, **poly-1** was ground to a fine powder using a motor and pestle before 200 mg was added to a 10 mL solution of $AuCl_3$ in water (100 ppm Au^{3+}). Au^{3+} was used as a model gold species as this oxidation state is formed with some oxidative lixiviants.[49] After rotating the mixture for 12 hours at ambient temperature, the gold concentration was measured by atomic absorption spectroscopy (AAS). More than 97% of the gold was captured by **poly-1** (Fig. 10A and S85-S86). The polymer-bound gold (a solid) was recovered by centrifugation and then analyzed by energy dispersive X-ray (EDX) spectroscopy. Gold was observed across the polymer surface, which is consistent with the coordination of the trisulfide to the gold salt (Fig. 10B). Next, the polymer-bound gold was heated to 170 °C for 12 hours to provoke depolymerization (Fig. 10C). After this time, the mixture was subjected to reduced pressure (15 mbar) for 3 hours to separate the regenerated monomer from the gold. The monomer was recovered in 70% yield and separated from the concentrated gold. Analytical digestion of the recovered gold with aqua regia and subsequent analysis by AAS indicated quantitative recovery of the gold from the original solution (S87-S89). With a good yield of the recovered monomer, more sorbent could be prepared and re-used, so this is a promising concept in gold sorption from leachates encountered in mining and e-waste recycling.

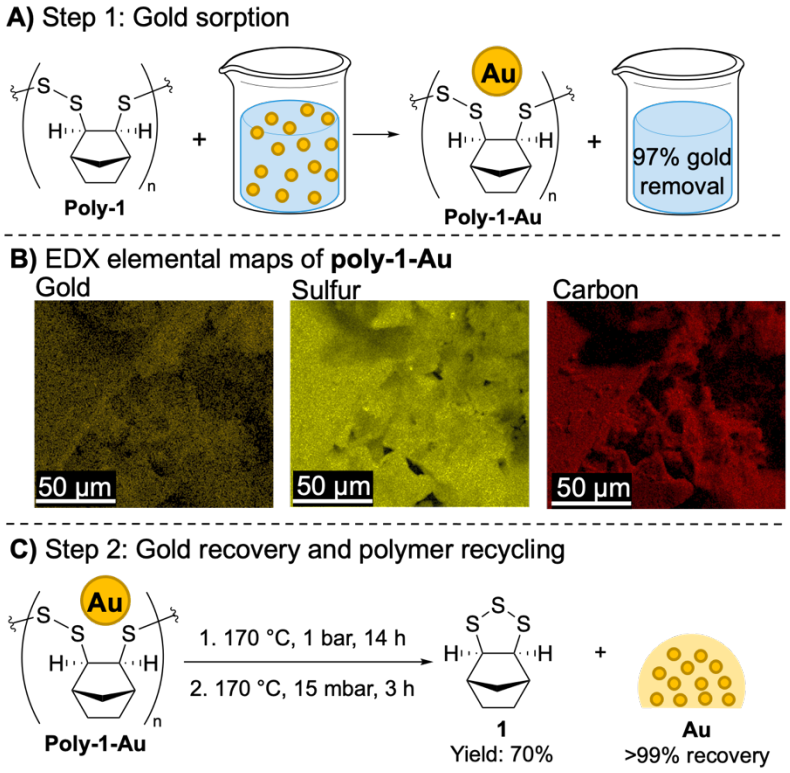

Figure 10: A) Poly-1 (200 mg) was added in powdered form to a 10 mL aqueous solution of $AuCl_3$ (100 ppm in Au^{3+}). After rotating 12 hours, 97% of the gold had been removed from the solution. **B)** Energy dispersive X-ray (EDX) spectroscopy of the isolated polymer, now bound to gold. Gold, sulfur and carbon are all co-located across the polymer, which was consistent with **poly-1** binding to Au^{3+} and removing it from the water. **C)** Heating the complex formed from

the polymer and gold (**poly-1-Au**) resulted in depolymerization and reformation of monomer **1**. The regenerated monomer was recovered by distillation in an isolated yield of 70%. The gold remained behind and was recovered in quantitative yield.

Copper binding

Poly-1, **poly-3** and **poly-4** were tested for their ability to bind to Cu(II). **Poly-3** was of particular interest due to its carboxylic acid functional groups. Carboxylates are commonly used donor sites for coordination with metals such as copper [50] and ionic polymers can have improved water solubility which may improve metal binding in aqueous solutions.[38] Therefore, **poly-3** was reacted with 1 molar equivalent of NaOH per carboxylic acid group to provide the water-soluble **Na poly-3** (S90-S91).

The four polymers were studied for their Cu(II) binding abilities using a 0.5:1 and 1:1 $CuSO_4$ to monomer ratio in water. After 1 hour, the results indicated that **Na poly-3** displayed the best Cu binding properties of the polymers tested with an 89% copper removal for the 0.5:1 copper to monomer ratio (Fig. 11A). The other polymers, which are not soluble in water, removed less than 33% of the Cu(II) present. The higher copper ratio of 1:1 also showed that **Na poly-3** had the highest affinity to Cu in solution with a removal of 51% while the remaining polymers showed a binding less than 40% (S91-S92). It is suspected that the improved binding of Cu to **Na poly-3** was a result of the combination of improved interaction with the metals in water as well as the presence of carboxylate groups that serve as ligands for copper. The binding percentages measured suggest that two carboxylate groups bind to one Cu metal. This form of binding causes cross-linking between polymer chains and precipitation of the polymer as a gel (Fig. 11B). This precipitation mechanism is useful when considering the use of **Na poly-3** as a flocculant in copper recovery processes or remediation applications.

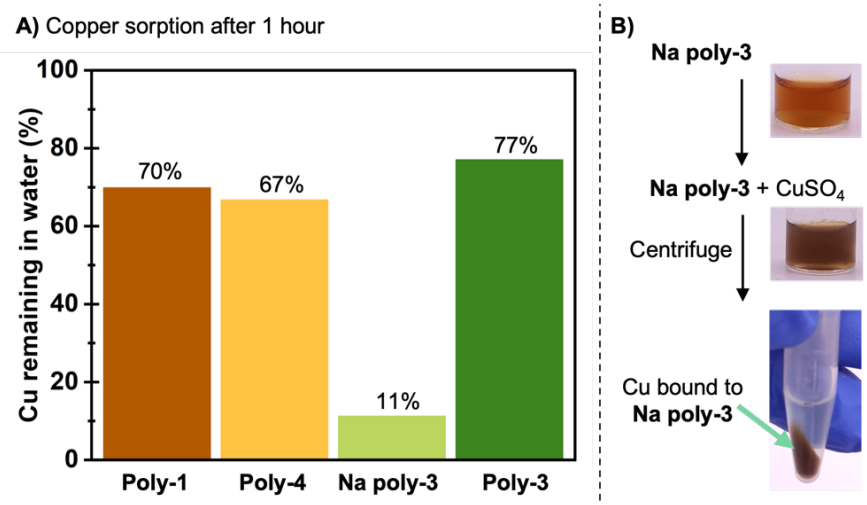

Figure 11: A) Copper sorption plot showing Cu remaining in solution of 0.5:1 Cu(II) to monomer ratios after 1 hour of agitation. **B)** Images showing fully soluble **Na poly-3** in H_2O, the addition

of $CuSO_4$ caused precipitation of the polymer as a gel, while simultaneously removing Cu from solution.

Thermal curing

Thermal curing of **poly-4** was investigated to test if cross-linking would provide a material that is more chemically and thermally robust than the linear polymer (S93-S94). This route also would provide a safe method for the synthesis and curing of sulfur-dicyclopentadiene co-polymers that are prone to runaway reactions when produced through inverse vulcanization.[26]

Poly-4 (250 mg) was cured at 190 °C for 6 hours, which caused it to turn from brown to black (Fig. 12A). The thermal stability of cured **poly-4** was studied using thermal gravimetric analysis (TGA) which shows a distinct change in initial mass loss at 235 °C compared to **poly-4** which begins degrading at 180 °C. Solvent stability studies showed cured **poly-4** was insoluble in THF and chloroform, whereas uncured **poly-4** was soluble in both (Fig. 12C). An increase in thermal stability and decrease in solubility suggests crosslinking during thermal curing due to S-S bond scission and addition of thiyl radicals to the alkene in **poly-4** (Fig. 12A).[51]

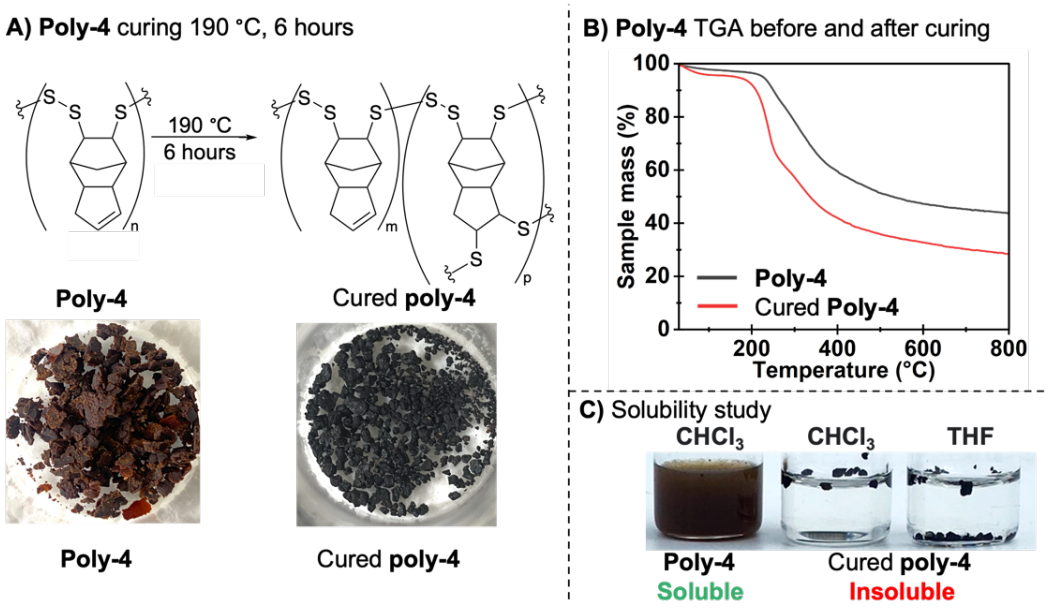

Figure 12: A) Images of **poly-4** before and after curing at 190 °C for 6 hours. **B)** TGA comparing **poly-4** and cured **poly-4**. **C) Poly-4** (10 mg) and cured **poly-4** (10 mg) in 1 mL of either chloroform or THF. **Poly-4** is soluble in chloroform and cured **poly-4** is insoluble in chloroform and THF.

CONCLUSIONS: The first electrochemically-initiated polymerization of cyclic trisulfides was developed. The reaction is safe and rapid at ambient temperature, providing sulfur-rich polymers with a well-defined sulfur rank of three. The electrochemical method is more robust

than analogous anionic polymerizations, which may motivate further uptake and exploration of this polymerization technique. Insight into the mechanism was provided by DFT calculations that revealed an intriguing self-correcting mechanism that favors propagation of the target trisulfide linkage. The product poly(trisulfide)s were used in several high-value applications including thermal depolymerization for monomer recycling, gold sorption and recovery, and copper binding and precipitation from water. More generally, because the monomers are prepared directly from elemental sulfur, this is a complementary strategy for conversion of excess elemental sulfur into value-added products. Unlike inverse vulcanization, however, the electrochemical polymerization is much milder and offers better control of sulfur-rank. Future studies will focus on the scope of this method, exploring new monomers, accessing other sulfur ranks, and preparing well-defined polysulfides with higher molecular weight and improved mechanical properties.

SUPPORTING INFORMATION: Full experimental and computational details as well as characterization data is supplied as electronic Supporting Information.

ACKNOWLEDGEMENTS: The authors acknowledge financial support from the Australian Research Council (DP200100090, LP200301660, LP200301661, FT220100054, DP210100025 and DP230100587). The authors also acknowledge the support of the Microscopy Australia research facility at Flinders University. This work was performed in part at the South Australian Node of the Australian National Fabrication Facility, established under the National Collaborative Research Infrastructure Strategy to provide micro and nanofabrication facilities for Australia's researchers. Part of this research were undertaken on the MX1[52] and MX2[53] beamlines at the Australian Synchrotron, Victoria, Australia. The authors also thank Anton Blencowe of the University of South Australia for assistance with aqueous GPC. MLC gratefully acknowledges generous allocations of supercomputing time on the National Facility of the Australian National Computational Infrastructure.

REFERENCES:

1. Chung, W. J.; Griebel, J. J.; Kim, E. T.; Yoon, H.; Simmonds, A. G.; Ji, H. J.; Dirlam, P. T.; Glass, R. S.; Wie, J. J.; Nguyen, N. A.; Guralnick, B. W.; Park, J.; Somogyi, A.; Theato, P.; Mackay, M. E.; Sung, Y.-E.; Char, K.; Pyun, J., The use of elemental sulfur as an alternative feedstock for polymeric materials. *Nat. Chem.* **2013,** *5*, 518-524.
2. Zhao, F.; Li, Y.; Feng, W., Recent Advances in Applying Vulcanization/Inverse Vulcanization Methods to Achieve High-Performance Sulfur-Containing Polymer Cathode Materials for Li-S Batteries. *Small Methods* **2018,** *2*, 1800156.

3. Crockett, M. P.; Evans, A. M.; Worthington, M. J. H.; Albuquerque, I. S.; Slattery, A. D.; Gibson, C. T.; Campbell, J. A.; Lewis, D. A.; Bernardes, G. J. L.; Chalker, J. M., Sulfur-Limonene Polysulfide: A Material Synthesized Entirely from Industrial By-Products and Its Use in Removing Toxic Metals from Water and Soil. *Angew. Chem. Int. Ed.* **2016,** *55*, 1714-1718.
4. Worthington, M. J. H.; Kucera, R. L.; Albuquerque, I. S.; Gibson, C. T.; Sibley, A.; Slattery, A. D.; Campbell, J. A.; Alboaiji, S. F. K.; Muller, K. A.; Young, J.; Adamson, N.; Gascooke, J. R.; Jampaiah, D.; Sabri, Y. M.; Bhargava, S. K.; Ippolito, S. J.; Lewis, D. A.; Quinton, J. S.; Ellis, A. V.; Johs, A.; Bernardes, G. J. L.; Chalker, J. M., Laying Waste to Mercury: Inexpensive Sorbents Made from Sulfur and Recycled Cooking Oils. *Chem. Eur. J.* **2017,** *23*, 16219-16230.
5. Wu, X.; Smith, J. A.; Petcher, S.; Zhang, B.; Parker, D. J.; Griffin, J. M.; Hasell, T., Catalytic inverse vulcanization. *Nat. Commun.* **2019,** *10*, 647.
6. Griebel, J. J.; Namnabat, S.; Kim, E. T.; Himmelhuber, R.; Moronta, D. H.; Chung, W. J.; Simmonds, A. G.; Kim, K.-J.; van der Laan, J.; Nguyen, N. A.; Dereniak, E. L.; MacKay, M. E.; Char, K.; Glass, R. S.; Norwood, R. A.; Pyun, J., New Infrared Transmitting Material via Inverse Vulcanization of Elemental Sulfur to Prepare High Refractive Index Polymers. *Adv. Mater.* **2014,** *26*, 3014-3018.
7. Kleine, T. S.; Glass, R. S.; Lichtenberger, D. L.; Mackay, M. E.; Char, K.; Norwood, R. A.; Pyun, J., 100th Anniversary of Macromolecular Science Viewpoint: High Refractive Index Polymers from Elemental Sulfur for Infrared Thermal Imaging and Optics. *ACS Macro Lett.* **2020,** *9*, 245-259.
8. Griebel, J. J.; Glass, R. S.; Char, K.; Pyun, J., Polymerizations with elemental sulfur: A novel route to high sulfur content polymers for sustainability, energy and defense. *Prog. Polym. Sci.* **2016,** *58*, 90-125.
9. Worthington, M. J. H.; Kucera, R. L.; Chalker, J. M., Green chemistry and polymers made from sulfur. *Green Chem.* **2017,** *19*, 2748-2761.
10. Chalker, J. M.; Worthington, M. J. H.; Lundquist, N. A.; Esdaile, L. J., Synthesis and Applications of Polymers Made by Inverse Vulcanization. *Top. Curr. Chem.* **2019,** *377*, 16.
11. Zhang, Y.; Glass, R. S.; Char, K.; Pyun, J., Recent advances in the polymerization of elemental sulphur, inverse vulcanization and methods to obtain functional Chalcogenide Hybrid Inorganic/Organic Polymers (CHIPs). *Polym. Chem.* **2019,** *10*, 4078-4105.
12. Lee, T.; Dirlam, P. T.; Njardarson, J. T.; Glass, R. S.; Pyun, J., Polymerizations with Elemental Sulfur: From Petroleum Refining to Polymeric Materials. *J. Am. Chem. Soc.* **2022,** *144*, 5-22.

13. Sheard, W.; Park, K. W.; Leitao, E. M., Polysulfides as Sorbents in Support of Sustainable Recycling. *ACS Sustainable Chem. Eng.* **2023,** *11*, 3557-3567.
14. Kutney, G., *Sulfur: History, Technology, Applications & Industry*. 2nd ed.; ChemTec Publishing: Toronto, 2013.
15. Apodaca, L. E., Sulfur. U.S. Geological Survey, Mineral Commodity Summaries, January 2022.
16. Tonkin, S. J.; Pham, L. N.; Gascooke, J. R.; Johnston, M. R.; Coote, M. L.; Gibson, C. T.; Chalker, J. M., Thermal imaging and clandestine surveillance using low-cost polymers with long-wave infrared transparency. *ChemRxiv* **2022**, DOI: 10.26434/chemrxiv-2022-bzzd3.
17. Chalker, J. M.; Mann, M.; Worthington, M. J. H.; Esdaile, L. J., Polymers Made by Inverse Vulcanization for Use as Mercury Sorbents. *Org. Mater.* **2021,** *3*, 362-373.
18. Griebel, J. J.; Nguyen, N. A.; Namnabat, S.; Anderson, L. E.; Glass, R. S.; Norwood, R. A.; MacKay, M. E.; Char, K.; Pyun, J., Dynamic Covalent Polymers via Inverse Vulcanization of Elemental Sulfur for Healable Infrared Optical Materials. *ACS Macro Lett.* **2015,** *4*, 862-866.
19. Xin, Y.; Peng, H.; Xu, J.; Zhang, J., Ultrauniform Embedded Liquid Metal in Sulfur Polymers for Recyclable, Conductive, and Self-Healable Materials. *Adv. Funct. Mater.* **2019**, 1808989.
20. Tonkin, S. J.; Gibson, C. T.; Campbell, J. A.; Lewis, D. A.; Karton, A.; Hasell, T.; Chalker, J. M., Chemically induced repair, adhesion, and recycling of polymers made by inverse vulcanization. *Chem. Sci.* **2020,** *11*, 5537-5546.
21. Mann, M.; Kruger, J. E.; Andari, F.; McErlean, J.; Gascooke, J. R.; Smith, J. A.; Worthington, M. J. H.; McKinley, C. C. C.; Campbell, J. A.; Lewis, D. A.; Hasell, T.; Perkins, M. V.; Chalker, J. M., Sulfur polymer composites as controlled-release fertilizers. *Org. Biomol. Chem.* **2019,** *17*, 1929-1936.
22. Valle, S. F.; Giroto, A. S.; Klaic, R.; Guimarães, G. G. F.; Ribeiro, C., Sulfur Fertilizer Based on Inverse Vulcanization Process with Soybean Oil. *Polym. Degrad. Stab.* **2019**, *162,* 102-105.
23. Fortuna do Valle, S.; Soares Giroto, A.; Gestal Reis, H. P.; Guimarães, G. G. F.; Ribeiro, C., Synergy of Phosphate-Controlled Release and Sulfur Oxidation in Novel Polysulfide Composites for Sustainable Fertilization. *J. Agric. Food Chem.* **2021,** *69*, 2392-2402.
24. Lundquist, N. A.; Yin, Y.; Mann, M.; Tonkin, S. J.; Slattery, A. D.; Andersson, G. G.; Gibson, C. T.; Chalker, J. M., Magnetic responsive composites made from a sulfur-rich polymer. *Polym. Chem.* **2022,** *13*, 5659-5665.

25. Mann, M.; Pauling, P. J.; Tonkin, S. J.; Campbell, J. A.; Chalker, J. M., Chemically activated S-S metathesis for adhesive-free bonding of polysulfide surfaces. *Macromol. Chem. Phys.* **2021**, 2100333.

26. Parker, D. J.; Jones, H. A.; Petcher, S.; Cervini, L.; Griffin, J. M.; Akhtar, R.; Hasell, T., Low cost and renewable sulfur-polymers by inverse vulcanization, and their potential for mercury capture. *J. Mater. Chem. A* **2017,** *5*, 11682-11692.

27. Griebel, J. J.; Li, G.; Glass, R. S.; Char, K.; Pyun, J., Kilogram scale inverse vulcanization of elemental sulfur to prepare high capacity polymer electrodes for Li-S batteries. *J. Polym. Sci., Part A: Polym. Chem.* **2015,** *53*, 173-177.

28. Lundquist, N. A.; Tikoalu, A. D.; Worthington, M. J. H.; Shapter, R.; Tonkin, S. J.; Stojcevski, F.; Mann, M.; Gibson, C. T.; Gascooke, J. R.; Karton, A.; Henderson, L. C.; Esdaile, L. J.; Chalker, J. M., Reactive compression molding post-inverse vulcanization: A method to assemble, recycle, and repurpose sulfur polymers and composites. *Chem. Eur. J.* **2020,** *26*, 10035-10044.

29. Zhang, Y.; Pavlopoulos, N. G.; Kleine, T. S.; Karayilan, M.; Glass, R. S.; Char, K.; Pyun, J., Nucleophilic Activation of Elemental Sulfur for Inverse Vulcanization and Dynamic Covalent Polymerizations. *J. Polym. Sci., Part A: Polym. Chem.* **2019,** *57*, 7-12.

30. Dodd, L. J.; Omar, Ö.; Wu, X.; Hasell, T., Investigating the Role and Scope of Catalysts in Inverse Vulcanization. *ACS Catal.* **2021,** *11*, 4441-4455.

31. Yan, P.; Zhao, W.; McBride, F.; Cai, D.; Dale, J.; Hanna, V.; Hasell, T., Mechanochemical synthesis of inverse vulcanized polymers. *Nat. Commun.* **2022,** *13*, 4824.

32. Jia, J.; Liu, J.; Wang, Z.-Q.; Liu, T.; Yan, P.; Gong, X.-Q.; Zhoa, C.; Chen, L.; Miao, C.; Zhoa, W.; Cai, S. D.; Wang, X.-C.; Cooper, A. I.; Wu, X.; Hasell, T.; Quan, Z.-J., Photoinduced inverse vulcanization. *Nat. Chem.* **2022,** *14*, 1249–1257.

33. Kang, K.-S.; Olikagu, C.; Lee, T.; Bao, J.; Molineux, J.; Holmen, L. N.; Martin, K. P.; Kim, K.-J.; Kim, K. H.; Bang, J.; Kumirov, V. K.; Glass, R. S.; Norwood, R. A.; Njardarson, J. T.; Pyun, J., Sulfenyl Chlorides: An Alternative Monomer Feedstock from Elemental Sulfur for Polymer Synthesis. *J. Am. Chem. Soc.* **2022,** *144*, 23044-23052.

34. Baran, T.; Duda, A.; Penczek, S., Anionic Polymerization of Norbornene Trisulfide (exo-3,4,5-Trithia-Tricyclo[5.2.1.0]decane). *J. Polym. Sci.* **1984,** *22*, 1085-1095.

35. Poulain, S.; Julien, S.; Duñach, E., Conversion of norbornene derivatives into vicinal-dithioethers via S^8 activation. *Tetrahedron Lett.* **2005,** *46*, 7077-7079.

36. Dodd, L. J.; Lima, C.; Costa-Milan, D.; Neale, A. R.; Saunders, B.; Zhang, B.; Sarua, A.; Goodacre, R.; Hardwick, L. J.; Kuball, M., Hasell, T. Raman analysis of inverse vulcanised polymers. *Polym. Chem.* **2023**, in press. DOI: 10.1039/D2PY01408D.

37. Rao, T. N.; Yagi, I.; Miwa, T.; Tryk, D. A.; Fujishima, A., Electrochemical Oxidation of NADH at Highly Boron-Doped Diamond Electrodes. *Anal. Chem.* **1999,** *71*, 2506-2511.
38. Eder, M. L.; Call, C. B.; Jenkins, C. L., Utilizing Reclaimed Petroleum Waste to Synthesize Water-Soluble Polysulfides for Selective Heavy Metal Binding and Detection. *ACS Appl. Polym. Mater.* **2022,** *4*, 1110-1116.
39. Alabi, O. A.; Ologbonjaye, K. I.; Awosolu, O.; Alalade, O. E., Public and Environmental Health Effects of Plastic Wastes Disposal: A Review. *J. Toxicol. Risk Assess.* **2019,** *5*, 021.
40. Grigore, M. E., Methods of Recycling, Properties and Applications of Recycled Thermoplastic Polymers. *Recycling* **2017,** *2*, 24.
41. Ragaert, K.; Delva, L.; Van Geem, K., Mechanical and chemical recycling of solid plastic waste. *Waste Manage.* **2017,** *69*, 24-58.
42. Rahimi, A.; García, J. M., Chemical recycling of waste plastics for new materials production. *Nat. Rev. Chem.* **2017,** *1*, 0046.
43. Zhang, X.; Fevre, M.; Jones, G. O.; Waymouth, R. M., Catalysis as an Enabling Science for Sustainable Polymers. *Chem. Rev.* **2018,** *118*, 839-885.
44. Miao, Y.; von Jouanne, A.; Yokochi, A., Current Technologies in Depolymerization Process and the Road Ahead. *Polymers* **2021,** *13*, 449.
45. Fortman, D. J.; Brutman, J. P.; De Hoe, G. X.; Snyder, R. L.; Dichtel, W. R.; Hillmyer, M. A., Approaches to Sustainable and Continually Recyclable Cross-Linked Polymers. *ACS Sustainable Chem. Eng.* **2018,** *6*, 11145-11159.
46. Esdaile, L. J.; Chalker, J. M., The Mercury Problem in Artisanal and Small-Scale Gold Mining. *Chem. Eur. J.* **2018,** *24*, 6905-6916.
47. Rao, M. D.; Singh, K. K.; Morrison, C. A.; Love, J. B., Challenges and opportunities in the recovery of gold from electronic waste. *RSC Adv.* **2020,** *10*, 4300-4309.
48. Mann, M.; Chalker, J. M., Materials and processes for recovering precious metals. WO2020198778. Priority date: 3 April 2019.
49. La Brooy, S. R.; Linge, H. G.; Walker, G. S., Review of gold extraction from ores. *Miner. Eng.* **1994,** *7*, 1213-1241.
50. Deacon, G.; Phillips, R., Relationships between the carbon-oxygen stretching frequencies of carboxylato complexes and the type of carboxylate coordination. *Coord. Chem. Rev.* **1980,** *33*, 227-250.
51. Mann, M.; Zhang, B.; Tonkin, S. J.; Gibson, C. T.; Jia, Z.; Hasell, T.; Chalker, J. M., Processes for coating surfaces with a copolymer made from sulfur and dicyclopentadiene. *Polym. Chem.* **2022,** *13*, 1320-1327.
52. Cowieson, N. P.; Aragao, D.; Clift, M.; Ericsson, D. J.; Gee, C.; Harrop, S. J.; Mudie, N.; Panjikar, S.; Price, J. R.; Riboldi-Tunnicliffe, A.; et al. MX1: A Bending-Magnet

Crystallography Beamline Serving Both Chemical and Macromolecular Crystallography Communities at the Australian Synchrotron. *J. Synchrotron Radiat.* **2015**, *22*, 187–190.

53. Aragao, D.; Aishima, J.; Cherukuvada, H.; Clarken, R.; Clift, M.; Cowieson, N. P.; Ericsson, D. J.; Gee, C. L.; Macedo, S.; Mudie, N.; et al. MX2: A High-Flux Undulator Microfocus Beamline Serving Both the Chemical and Macromolecular Crystallography Communities at the Australian Synchrotron. *J. Synchrotron Radiat.* **2018**, *25*, 885–891.